from Dissociative Recombination of Molecular Ions with Electrons, ed. by S. L. Guberman (Kluwer/Plenum Academic Press, New York, 2003), p. 187.

The Dissociative Recombination of N_2^+

Rate Coefficients and Isotope Effects

Steven L. Guberman
Institute for Scientific Research, 22 Bonad Road, Winchester, MA 01890
slg@sci.org

1. INTRODUCTION

The dissociative recombination (DR) of N_2^+,

$$N_2^+ + e^- \rightarrow N + N, \qquad (1)$$

plays a central role in determining the chemical and physical properties of planetary ionospheres. At 300 km above the surface of the Earth, DR is a well known loss process[1] for N_2^+ and an important source of excited N. Reaction (1) yields as much N(^{2}D) near 300 km as all other sources combined.[2] The dayglow emissions at 3466Å and 10,400Å due to N(^{2}P) arise in part from the DR of N_2^+. At Mars, DR of $^{14}N_2^+$ imparts sufficient kinetic energy to the product atoms to allow for atmospheric escape. However, in DR of $^{15}N^{14}N^+$ from v=0, although ^{14}N can escape the atmosphere, ^{15}N receives insufficient energy for escape.[3] This mechanism may explain why the Viking missions to Mars found $^{15}N/^{14}N$ to be 1.6 times greater than the value at Earth.[4] (Escape of N by DR of N_2^+ is not energetically possible at Earth.) DR of N_2^+ may also contribute to $^{15}N/^{14}N$ isotope enrichment at Titan.[5]

Here, I describe theoretical quantum chemical calculations of the DR cross sections and rate coefficients for the lowest three ion vibrational levels. The calculation of the potential curves needed to describe the DR of these three levels is described in the next section. In Section 3, the calculation of the electronic widths is described. A description of the calculation of the rate coefficients and a comparison to experimental values are in Section 4. Isotope effects are discussed in Section 5. The results are summarized in Section 6.

2. POTENTIAL CURVES AND MECHANISMS

The calculation of rates coefficients for Reaction (1) requires an accurate description of the potentials that describe the motion of the ion nuclei and the dissociating neutral atoms. For DR from the first excited ion vibrational level at low electron energies (e.g. < 1 eV), 5 atomic asymptotes are energetically accessible: $^4S + {}^4S$, $^4S + {}^2D$, $^4S + {}^2P$, $^2D + {}^2D$, and $^2D + {}^2P$. A total of 90 molecular states arise from these asymptotes. At first glance the problem seems somewhat daunting since for DR it is necessary to determine which of these states cross the ion near the turning points for the v=0,1 vibrational levels. However, molecular symmetry considerations allow for the elimination of many states. For example, since the ion is of $^2\Sigma_g^+$ symmetry, only singlet and triplet spin states can be formed after electron capture. Therefore, all states of septet and quintet symmetry can be eliminated. States of negative reflection symmetry also cannot be formed by electron capture. In order to identify the important states, small scale Complete Active Space Self Consistent Field (CASSCF)[6] calculations were done. These calculations and the larger scale calculations were done with nuclear centered contracted Gaussian basis sets. For these calculations, I have used the [5s, 4p, 3d, 2f, 1g] basis of Dunning.[7] Here the letters represent the angular momenta of the basis functions and the numbers are the number of contracted Gaussian functions. Each contracted Gaussian is a superposition of individual Gaussians with optimized contraction coefficients and exponents.

The description of DR used here involves potential curves that describe diabatic states. The states are diabatic because they intentionally exclude Rydberg character from the basis set. The exclusion is needed in order to allow the repulsive states to cross the ion. The electrostatic widths described in the next Section are consistent with this use of diabatic states. Alternatively, fully optimized states including Rydberg character could have been used. In this case, the widths are not electrostatic but instead are Born-Oppenheimer coupling matrix elements. None of the repulsive curves cross through the ion in this case. However, for the N_2 potential curves, the diabatic approach is the most convenient.

The CASSCF calculations identified 25 states that were candidates for large scale calculations. The large scale calculations used the CASSCF orbitals in Contracted Multireference Configuration Interaction (CMRCI)[8] calculations for the potential curves. The detailed results of these calculations will be reported separately. For seven states of N_2 for which there are experimental values for comparison,[9,10] the average differences between experimental and calculated excitation energies, force constants and equilibrium internuclear separations are only 0.04 eV, 22 cm^{-1}, and 0.019 Bohr respectively.

For v=0, the CMRCI potential curves which intersect the ion within or

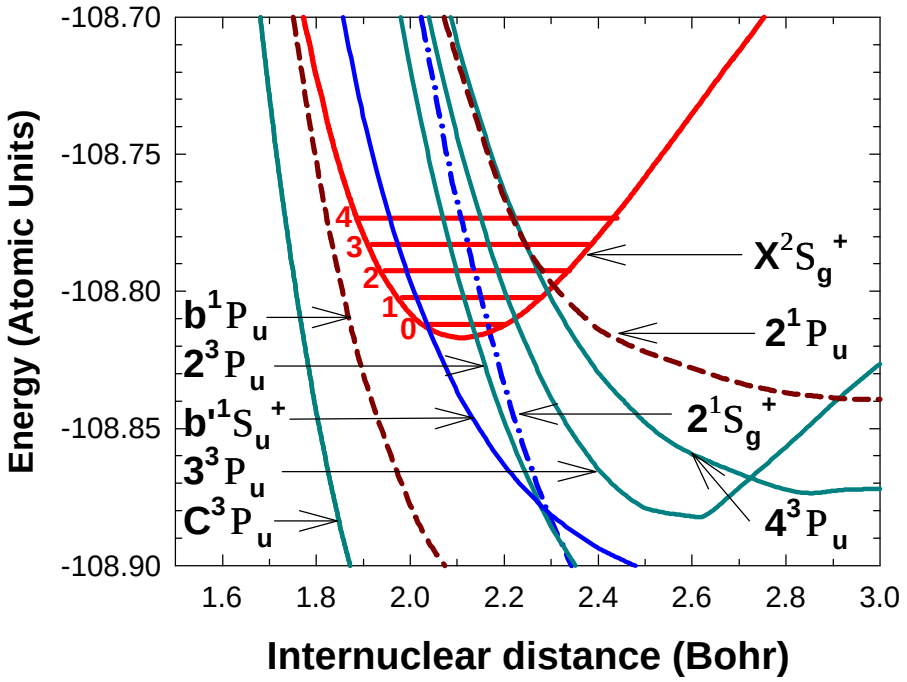

Figure 1. Ion and dissociative potential curves for N_2^+ DR of v=0 and 1.

near the endpoints of the vibrational motion are shown in Fig. 1 and are $2^3\Pi_u$, $3^3\Pi_u$, $2^1\Sigma_g^+$, and $b\mathbb{N}^1\Sigma_u^+$. For the v=1 level, the important states are those for v=0 plus $4^3\Pi_u$ and $2^1\Pi_u$. Several additional states with favorable intersections are not shown in Fig. 1 because they have very small electron capture widths (see next Section). The $^3\Pi_u$ curves are the same as those reported earlier[11,12] and were calculated in a [4s, 3p, 2d, 1f] basis. These curves have been shifted in energy in order to plot them on the same Figure with curves calculated in the larger basis set.

The $b\mathbb{N}^1\Sigma_u^+$ curve crosses the ion curve at the inner turning point of v=0 and leads to N(^{2}P) + N(^{2}D) atoms which are not energetically accessible from v=0 until the electron energy is above 0.137 eV. Therefore, this state will not affect room temperature rate constants. Below 0.137 eV electron energy, DR along this route is energetically possible for the excited vibrational levels.

Dissociative routes that do not cross within the ion vibrational turning points may also be important for DR via the indirect mechanism. Capture into a highly excited vibrational level of a Rydberg state can lead to predissociation along a repulsive curve that is not near the ion. While this mechanism does occur in N_2^+ DR, its magnitude is not large enough to affect the values for the rate constants reported below.

Additional potential curves included in the rate coefficient calculations

(see below) are the Rydberg series having the same symmetry as each of the important dissociative states identified above. In addition, the rate coefficient calculations include the $^3\Pi_u$ states having the $A^2\Pi_u$ excited ion core.[12] These curves were determined from the quantum defects that were in turn determined in the width calculations (see next Section).

Because there is more than one $^3\Pi_u$ state that takes part in DR, a very interesting mechanism occurs here.[13] Since the $^3\Pi_u$ dissociative states predissociate the same set of $^3\Pi_u$ Rydberg states, the Rydberg states can be viewed as intermediates that "connect" the two dissociative states. In a time independent picture, the dissociative states mix with each other due to the Rydberg states. In a time dependent picture, the flux proceeding along one dissociative state can transfer to another state of the same symmetry prior to dissociation or autoionization. This mechanism allows for dissociation along a route that does not have a favorable intersection with the ion if capture can occur into a repulsive state of the same symmetry that has a favorable crossing. Fig. 1 shows that initial electron capture into $2^3\Pi_u$ can be followed in part by dissociation along $3^3\Pi_u$ and $4^3\Pi_u$. A similar mechanism can also connect repulsive states of different electronic symmetry. An example is the DR of O_2^+ leading to $O(^1S)$ where spin-orbit coupling connects two dissociative states[14] via connected Rydberg states. The effect of the spin-orbit coupling is quite dramatic and amounts to over an order of magnitude increase in the DR rate coefficient. However, the spin-orbit coupling mechanism requires that the ion have both nonzero angular momentum and spin projection on the internuclear axis. Therefore, this mechanism does not occur in the DR of N_2^+ $X\,^2\Sigma_g^+$ but can occur in the DR of N_2^+ excited states.

3. ELECTRONIC WIDTHS

The probability of electron capture and autoionization is governed by an electronic width, $\Gamma(R)$. The direct DR cross section is approximately directly proportional to $\Gamma(R)$, which is given by the Golden Rule expression,

$$\Gamma_{r,d}(R)=2\pi D<\{M_{ion}(x,R)N_r(x,R)\}|H|M_d(x,R)>^2. \quad \textbf{(2)}$$

In (2), H is the electronic Hamiltonian, R is the internuclear distance, the integration is over the electronic coordinates represented by x, and the electronic wave functions from left to right are for the ion core, the Rydberg electron, and the dissociative neutral state. The antisymmetrized product of the ion core and Rydberg electron wave functions is denoted by {} and the density of states is given by D.

The calculation of the width has been described previously[15-17] and involves the placement of a large basis set of diffuse Gaussians[18] at the

molecular midpoint coupled with the use of the Improved Virtual Orbital (IVO) method for calculating the Rydberg orbitals.[19] These calculations allow for the accurate description of a Rydberg series having principal quantum numbers as high as n=10. The width is calculated as in (2) with high Rydberg orbitals used to represent the free electron. The matrix element is then multiplied by a density of states factor in order to convert the normalization of the Rydberg orbital to that for a continuum coulomb-like orbital. The wave functions for the ion and dissociative states in (2) are full valence space CI wave functions. The full Rydberg state wave function is obtained by coupling the Rydberg orbitals determined in the IVO procedure with the ion multiconfiguration wave function. In addition, the multiconfiguration wave function for the ion plus a Rydberg electron is allowed to mix in higher nonphysical correlating roots from the space of configurations describing the dissociating states. This procedure allows important additional correlation to mix into the electron-ion states[15,20]

From the energy difference, $\Delta E(R)$, between the multiconfiguration Rydberg and ion wave functions, the quantum defect, $\mu(R)$, is calculated. The quantum defect is given by $\mu(R) = n - (1/(2\ \Delta E(R)))^{½}$ where n is the principal quantum number. The quantum defect is an important input parameter for the calculation of the cross sections and rate coefficients.

An example of the calculated widths (from Eq.(2)) for a full range of effective principal quantum numbers, n* (where $n^*=n-\mu$), is given in Fig. 2 for the C and $2^3\Pi_u$ states. In both cases, the widths must be determined up to n* 9 in order to assure convergence to two significant figures.

4. RATE COEFFICIENTS

For the calculation of DR cross sections, we use the Multichannel Quantum Defect Theory (MQDT) approach.[17,21] This approach allows one to treat direct and indirect DR simultaneously in order to accurately describe the important interference between these processes. In this approach, an electronic matrix is constructed which takes into account the interactions between all channels. Using the width matrix elements in Eq.(2), the matrix elements of the electronic interaction matrix or K matrix can be calculated. The first order matrix elements are[21]

$$K_{ion,d} = (1/2B)^{1/2} < X_{ion} \mid \Gamma_{r,d}^{1/2}(R) \mid X_d > , \qquad (3)$$

where X_{ion} and X_d are vibrational wave functions for the ion and dissociative states respectively, Γ is from Eq. (2), and the integration in (3) is over the internuclear distance, R. Higher order contributions to this matrix element are also included.[17] These contributions include the second order electronic

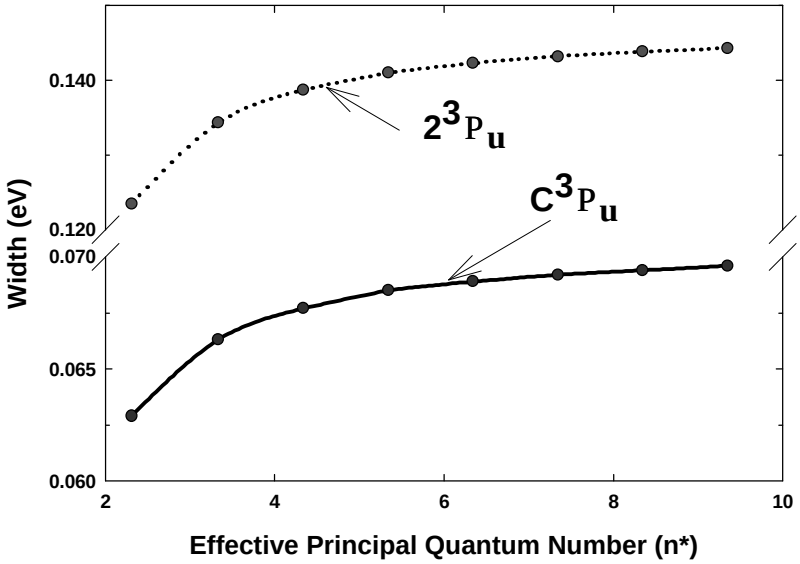

Figure 2. Electronic widths from Eq.(2) for two states of N_2.

coupling, which has already been described in the first chapter of this volume. In addition, the excitation of vibrationally excited intermediate neutral Rydberg states (indirect DR) by Born-Oppenheimer breakdown is included as is the interference between all these processes. The eigenvalues and eigenvectors obtained from the diagonalization of the K matrix are used to construct frame transformation matrix elements from which the scattering matrix can be determined by a method due to Seaton.[22] The cross sections and rate coefficients are calculated from the energy dependent scattering matrix. For the $^3\Pi_u$ cross sections, the K matrix includes 18 vibrational levels in the ion ground state and 18 in the $A^2\Pi_u$ excited core state. With the dissociative states, the K matrix is 40x40 for $^3\Pi_u$. For each of the remaining states shown in Fig. 1, excited core states are not included. For $^1\Pi_u$, the K matrix is 20x20. For the remaining states, the K matrices are 19x19. The ℓ=1 π partial waves for the 'free' electron are included.

The calculated rate coefficients for the lowest three vibrational levels of N_2^+ are shown in Table 1. The rate coefficients are obtained by Maxwellian averaging of the calculated cross sections. The coefficient for v=0 at 300 K is $2.1 \times 10^{-7} \times (T_e/300)^{-0.20}$ cm^3/sec. The previously reported calculated coefficient, $(1.6 \times 10^{-7} \times (T_e/300)^{-0.37} cm^3/sec)$,[11] is for a single dissociative route, $2^3\Pi_u$. The 300K rate coefficient is in excellent agreement with experimental results,[23-25] which range from $1.70\pm0.09 \times 10^{-7} \times (T_e/300)^{-0.30\pm0.09} cm^3/sec$[23] to $2.6\times10^{-7} cm^3/sec$.[24] This agreement gives us confidence that the calculated results for v=1 and 2 can also be expected to be

Several incorrect rate constants in the original paper are corrected on this page.

	Electron Temperature (K)	
v	300	800
0	2.1 x $(T_e/300)^{-0.20}$	1.6 x $(T_e/800)^{-0.37}$
1	1.9 x $(T_e/300)^{-0.87}$	0.81 x $(T_e/800)^{-0.78}$
2	1.3 x $(T_e/300)^{-0.49}$	0.96 x $(T_e/800)^{-0.29}$

Table 1. Total Calculated DR rate coefficients (x 10^7) for N_2^+.

quite accurate. For excited vibrational levels, there are no experimental measurements or prior theoretical calculations. However, the most recent storage ring results indicate that the rate coefficients are not "strongly dependent" upon vibrational level.[23] The calculations reported here indicate otherwise (except for v=0,1 at 300K). At 300 K, the calculated rate coefficient for v=2 is about 38% lower than that for v=0. At 800K (ionospheric temperature), the v=0 and 1 rate coefficients differ by 49%. For v=2, the calculated rate coefficient is 40% below that for v=0 at 800K. For each vibrational level, the DR rate coefficient decreases with increasing electron temperature. One can show that if the total effective (over several dissociative states) Franck-Condon factor (between the dissociative and bound vibrational levels) remains constant as the electron energy increases, the rate coefficient will have a temperature dependence of $T_e^{-0.50}$. The values of the exponents for the temperature dependencies of the v=0 and 2 rate coefficients are more positive than -0.50 indicating that the effective Franck-Condon factors increase with electron energy. However, for v=1 the exponents indicate that the Franck-Condon factor decreases with increasing electron energy.

An analysis of Atmosphere Explorer data,[26] led to the proposal that the DR rate coefficient from excited vibrational levels had to be high, i.e. about 1.7 x 10^{-6} for v=1 at electron temperatures between 1400 and 2400K, in order to explain why the measured N_2^+ density was lower than expected. At these temperatures, my calculations give a rate coefficient of 0.46 x 10^{-7} x $(T_e/1900)^{-0.57}$ cm^3/sec for v=1 and 1.1 x 10^{-7} x $(T_e/1900)^{-0.54}$ cm^3/sec for v=0. The proposal[26] that the rate constant for v=1 may be 1.7 x 10^{-6} cm^3/sec at these electron temperatures, is not supported by these results. However, the final word rests with calculations currently underway, in which all of the core excited Rydberg states are included. Nevertheless, it is unlikely that the calculated rate coefficients will increase by an order of magnitude. Instead, other aspects of the model that predicts the N_2^+ density will have to be reexamined in order to understand the disagreement between the model results and the measurements. Objections, supported by these calculations, have been raised concerning the possibility of very high DR rate coefficients from excited vibrational levels.[27]

5. ISOTOPIC SUBSTITUTION

Isotopic substitution is an important issue because recent storage ring experiments[28] have used $^{15}N^{14}N^+$ instead of $^{14}N_2^+$ to measure DR rate coefficients and quantum yields. The rationale for using $^{15}N^{14}N^+$ is that due to its small dipole moment, it may vibrationally relax in a storage ring prior to DR and thereby guarantee that DR from only v=0 is being measured. However, $^{14}N_2^+$ has no dipole moment and will not radiatively relax within the duration of the experiment. Unfortunately, the measurements[28] show that even $^{15}N^{14}N^+$ is not relaxed prior to recombination. Are the storage ring measurements of rate coefficients for $^{15}N^{14}N^+$ relevant to the $^{14}N_2^+$ found in ionospheres?

Using the same approach described above, for the DR of $^{15}N^{14}N^+$ I find that the total DR rate coefficient at 300K from v=0 is 26% higher than the corresponding rate coefficient for $^{14}N_2^+$ (2.1 x 10^{-7} cm^3/sec). At an ionospheric temperature of 1000K, the $^{15}N^{14}N^+$ DR rate coefficient is 11% higher than the $^{14}N_2^+$ value (1.43 x 10^{-7} cm^3/sec). However, the storage ring DR experiment[28] on $^{15}N^{14}N^+$ has reported quantum yields at only T_e = 0 K where the rate coefficient is expected to differ by more than 26% from the $^{14}N_2^+$ value. Future work is needed to determine if there may be a fortuitous cancellation of errors in calculating the quantum yields for $^{14}N_2^+$ from the data for $^{15}N^{14}N^+$. In the mean time, the experimental $^{15}N^{14}N^+$ yields should be used with caution when modeling the $^{14}N_2^+$ ionospheric chemistry.

6. SUMMARY

Quantum theoretical calculations have been completed for the DR of N_2^+ from the lowest three ion vibrational levels. The calculated rate coefficient from v=0 agrees well with experimentally determined values. However, at room temperature, the calculated v=1 rate coefficient is 38% higher than that for v=0. The v=2 rate coefficient is about ½ of the v=0 value. These results contrast with recent storage ring experiments[23] where different ion vibrational distributions generated in different ion sources were studied. The results indicated that the rate coefficients would have little variation with v. Calculations on $^{15}N^{14}N^+$, show that at room temperature, the rate coefficient for v=0 DR is 26% higher than that for $^{14}N_2^+$, with the difference decreasing as the electron temperature increases. While the DR rate coefficients are considerably different for the two isotopomers at room temperature and below, it is not clear if this difference also holds for the quantum yields. Quantum yield calculations, in progress in this laboratory, will answer this question.

ACKNOWLEDGEMENTS

This material is based upon work supported by the National Science Foundation under Grants ATM-9812034 and ATM-0225256. The research was also supported by NASA Grants NAG5-12220, NAG5-11827, and NAG5-11428.

REFERENCES

1 M. R. Torr and D. G. Torr, Geophys. Res. Lett. **6**, 775 (1979).
2 J. E. Frederick and D. W. Rusch, J. Geophys. Res. **82**, 3509 (1977).
3 J. L. Fox and A. Haæ, J. Geophys. Res. **102**, 9191 (1997).
4 A. O. Nier, M. B. McElroy and Y. L. Yung, Science **194**, 68 (1976); M. B. McElroy, Y. L. Yung and A. O. Nier, Science **194**, 70 (1976).
5 H. Lammer, W. Stumptner, G. J. Molina-Cuberos, S. J. Bauer, T. Owen, Planet. Space Sci. **48**, 529 (2000).
6 P. J. Knowles, and H.- J. Werner, Chem. Phys. Lett. **115**, 259 (1985); H.-J Werner and P. J. Knowles, J. Chem. Phys. **82**, 5053 (1985).
7 T. H. Dunning Jr., J. Chem. Phys. **90**, 1007 (1989).
8 H.- J. Werner and P. J. Knowles, J. Chem. Phys. **89**, 5803 (1988); P. J. Knowles and H.-J. Werner, Chem. Phys. Lett. **145**, 514 (1988). All calculations in the [54321] basis were done with the MOLPRO programs. MOLPRO is a package of ab initio programs written by H.- J. Werner and P. J. Knowles, with contributions from J. Almlöf, R. D. Amos, M. J. O. Deegan, S. T. Elbert, C. Hampel, W. Meyer, K. Peterson, R. Pitzer, A. J. Stone, P. R. Taylor, and R. Lindh.
9 A. Lofthus and P. H. Krupenie, J. Phys. Chem. Ref. Data **6**, 113 (1977).
10 K. P. Huber and G. Herzberg, *Molecular Spectra and Molecular Structure. IV Constants of Diatomic Molecules* (Van Nostrand Reinhold, New York, 1979).
11 S. L. Guberman, Geophys. Res. Lett. **18**, 1051 (1991).
12 S. L. Guberman, New Mechanisms for Dissociative Recombination, in *The Physics of Electronic and Atomic Collisions, XIX International Conference*, Book of Invited Papers, ed. by L. J. Dube et al. (American Institute of Physics Press, New York, 1995), p.307.
13 S. L. Guberman, Electron-Ion Continuum-Continuum Mixing in Dissociative Recombination, in *Dissociative Recombination: Theory, Experiment, and Applications*, ed. by B. R. Rowe, J. B. A. Mitchell, and A. Canosa (Plenum, New York, 1993), p.47.
14 S. L. Guberman, Science **278**, 1276 (1997).
15 S. L. Guberman, Ab Initio Studies of Dissociative Recombination, in *Dissociative Recombination: Theory, Experiment, and Applications*, ed. by J. B. A. Mitchell and S. L. Guberman (World Scientific, Singapore, 1989), p. 45. An extrapolation of the width to the continuum is no longer used.
16 S. L. Guberman, J. Chem. Phys. **102**, 1699 (1995).
17 S. L. Guberman and A. Giusti-Suzor, J. Chem. Phys. **95**, 2602 (1991).
18 K. Kaufmann, W. Baumeister and M. Jungen, J Phys. B **22**, 2223 (1989).
19 W. J. Hunt and W. A. Goddard III, Chem. Phys. Lett. **3**, 414 (1969).
20 A. U. Hazi, Molecular Resonance Phenomena, in *Electron-Atom and Electron-Molecule Collisions*, ed. by J. Hinze (Plenum Press, New York, 1983), p.103.
21 A. Giusti, J. Phys. B **13**, 3867 (1980).
22 M. J. Seaton, Rep. Prog. Phys. **46**, 167 (1983).

23 J. R. Peterson, A. Le Padellec, H. Danared, G. H. Dunn, M. Larsson, Å. Larson, R. Peverall, C. Strömholm, S. Rosén, M. af Ugglas and W. J. van der Zande, J. Chem. Phys. **108**, 1978 (1998).
24 A. Canosa, J. C. Gomet, B. R. Rowe and J. L. Queffelec, J. Chem. Phys. **94**, 7159 (1991).
25 F. J. Mehr and M. A. Biondi, Phys. Rev. **181**, 264 (1969); E. C. Zipf,, Geophys. Res. Lett. **7**, 645 (1980); M. Geoghegan, N. G. Adams and D. Smith, J. Phys. B **24**, 2589 (1991).
26 N. Orsini, D. G. Torr, H. D. Brinton, L. H. Brace, W. B. Hanson, J. H. Hoffman and A. O. Nier, Geophys. Res. Lett. **4**, 431 (1977).
27 M. A. Biondi, Geophys. Res. Lett. **5**, 661 (1978).
28 D. Kella, P. J. Johnson, H. B. Pedersen, L. Vejby-Christensen and L. H. Andersen, Phys. Rev. Lett. **77**, 2432 (1996).